Mon. Not. R. Astron. Soc. **000**, 000–000 (0000) Printed 13 May 2015 (MN LATEX style file v2.2)

Reionization constraints on primordial magnetic fields

Kanhaiya L. Pandey[1⋆], T. Roy Choudhury[1], Shiv K. Sethi[2] and Andrea Ferrara[3]
[1]*National Centre for Radio Astrophysics, TIFR, Pune 411007, India*
[2]*Raman Research Institute, Bangalore 560080, India*
[3]*Scuola Normale Superiore, Piazza dei Cavalieri 7, I-56126 Pisa, Italy*

13 May 2015

arXiv:1410.0368v2 [astro-ph.CO] 11 May 2015

ABSTRACT
We study the impact of the extra density fluctuations induced by primordial magnetic fields on the reionization history in the redshift range: $6 < z < 10$. We perform a comprehensive MCMC physical analysis allowing the variation of parameters related to primordial magnetic fields (strength, B_0, and power-spectrum index $n_{\rm B}$), reionization, and ΛCDM cosmological model. We find that magnetic field strengths in the range: $B_0 \simeq 0.05$–0.3 nG (for nearly scale-free power spectra) can significantly alter the reionization history in the above redshift range and can relieve the tension between the WMAP and quasar absorption spectra data. Our analysis puts upper-limits on the magnetic field strength $B_0 < 0.358, 0.120, 0.059$ nG (95 % c.l.) for $n_{\rm B} = -2.95, -2.9, -2.85$, respectively. These represent the strongest magnetic field constraints among those available from other cosmological observables.

Key words: dark ages, reionization, first stars – intergalactic medium – cosmology: theory – large-scale structure of Universe.

1 INTRODUCTION

Magnetic fields are ubiquitously present in the universe and play an important role in various astrophysical processes: star formation, accretion disks, proto-planetary disks, formation and stability of jets, dynamics of inter stellar medium (ISM), etc. (e.g. Parker 1979, Zeldovich, Ruzmaikin, & Sokolov 1983) However their role is still not well understood on larger scales and in the cosmological context, e.g. in the process of formation of the early galaxies and structure formation (e.g. Widrow 2002, Ryu et al. 2012). At present, the possible impact of cosmic magnetic fields is being investigated for a host of observables in astrophysics and cosmology. The probe of such fields is also one of the principle aims of many of the ongoing and upcoming large radio interferometers such as LOFAR[1] and SKA[2].

Magnetic fields in the universe are known to be coherent over the scales of galaxies and galaxy clusters, $\simeq$ 10–50 kpc (e.g. Beck 2012, Widrow 2002). There is also evidence of coherent magnetic fields over super-cluster scales (Kim et al. 1989). These fields could have arisen from the dynamo amplification of very small seed fields ($\simeq 10^{-20}$ G) generated in the early universe (e.g. Beck 2012). Alternatively, the observed fields might owe their origin to far stronger large scale primordial fields ($\sim 10^{-9}G$) that could have been generated during inflation or other an early phase transition in the universe (Turner & Widrow 1988, Ratra 1992, Widrow 2002, Ashoorioon & Mann 2005). Here we study some implications of the latter hypothesis.

Primordial magnetic fields leave their signature on a range of cosmological processes and observables (e.g. Yamazaki et al. 2012, Yamazaki 2014). These fields can generate density perturbations in addition to the ΛCDM model in the post-recombination epoch (Wasserman 1978, Kim, Olinto, & Rosner 1996, Gopal & Sethi 2003). The matter power spectrum of these density perturbations dominates the standard ΛCDM matter power spectrum at small scales ($\simeq$ 1–10 $\rm h^{-1}$ Mpc). Such effects can be directly probed by cosmological gravitational lensing and Lyman-α observations (Chongchitnan & Meiksin 2014, Pandey & Sethi 2013, Pandey & Sethi 2012, Shaw & Lewis 2012).

This additional power can cause early formation of structures (e.g., galaxies) which consequently cause early reionization of the IGM. As of today, the main observational constraints on reionization come from the CMB polarization data (e.g., those from the WMAP and Planck experiments, Planck Collaboration et al. 2013a) and the quasar absorption spectra at $z \gtrsim 5.5$ (Fan et al. 2006). Detailed models which are able to match these and a variety of other observations predict the reionization to be process extended over $6 \lesssim z \lesssim 15$. It has been shown that the presence of magnetic fields can affect the reionization history and alter the HI signal from epoch of reionization (Yamazaki et al. 2012, Sethi & Subramanian 2009, Kahniashvili et al. 2010, Sethi & Subramanian 2005). In this paper, we extend available detailed models of reionization (Choudhury & Ferrara 2005, Choudhury & Ferrara 2006) by

⋆ Email: kanhaiya@ncra.tifr.res.in
[1] http://www.lofar.org/
[2] https://www.skatelescope.org/

© 0000 RAS

including magnetic fields and carry out a detailed mutliparameter MCMC analysis to compare with available data sets. The main goal is to check the level of constraints one can put on the primordial magnetic field.

There is another aspect related to the magnetic fields, early formation of galaxies and reionization which is worth considering. Models which are consistent with all available data sets usually require some efficient sources of ionizing photons at high redshifts, e.g., metal-free PopIII stars (Choudhury & Ferrara 2005; Mitra, Choudhury, & Ferrara 2011) in addition to the usual PopII stars. These PopIII sources, however, are unlikely to contribute significantly to the photon budget at lower redshifts $z \lesssim 9$ because of feedback effects, which is crucial in matching the low photoionization rate inferred from quasar absorption spectra $z \sim 6$ (Bolton & Haehnelt 2007). One can thus conclude that in order to match the data sets, one requires a high ionizing emissivity at $z \sim 10$ which should preferably decrease by $z \sim 6$. In this regard, the presence of magnetic fields may assist in producing large number of dark matter haloes at high redshifts, and hence would help in reconciling with data sets without invoking any other sources like PopIII stars. This paper considers the effect of primordial magnetic field on the structure formation as a viable source which can affect the reionization process appreciably.

The plan of the paper is as follows: we discuss the model of reionization and the impact of the inclusion of primordial magnetic field in the next section. The main results are presented in Section 3. We summarize our results and discuss their implications in section 4.

2 METHOD

We first briefly summarize the main features of the reionization model used in this paper; the details can be found in Choudhury & Ferrara (2005), Choudhury & Ferrara (2006) and Choudhury (2009). The model follows the ionization and thermal histories of neutral, HII and HeIII regions simultaneously and self-consistently accounting for the IGM inhomogeneities based on a method outlined in Miralda-Escudé, Haehnelt, & Rees (2000). The density distribution of the IGM is assumed to be lognormal. The rate of number of ionizing photons per unit volume (i.e., ionizing emissivity) in the IGM from galaxies is assumed to be given by

$$\dot{n}_{\rm ph}(z) = n_b N_{\rm ion} \frac{{\rm d}f_{\rm coll}}{{\rm d}t}, \quad (1)$$

where n_b is the number density of baryons and $f_{\rm coll}$ is the dark matter collapsed fraction. The proportionality constant $N_{\rm ion}$ physically represents the number of ionizing photons in the IGM per baryon in collapsed objects. It can be written as

$$N_{\rm ion} = \epsilon_* f_{\rm esc} m_p \int_{\nu_{\rm HI}}^{\infty} {\rm d}\nu \left[\frac{{\rm d}N_\nu}{{\rm d}M_*}\right], \quad (2)$$

where ϵ_* is the fraction of baryons within collapsed haloes going into stars, $f_{\rm esc}$ is the escape fraction of ionizing photons and $[{\rm d}N_\nu/{\rm d}M_*]$ gives the number of ionizing photons (i.e., those with frequencies higher than the ionization threshold $\nu_{\rm HI}$) per frequency interval per unit stellar mass and is determined by the stellar IMF and the corresponding stellar spectra, m_p is proton-mass. We assume the stars to be Population II with subsolar metallicity $Z = 0.001 = 0.05 Z_\odot$ with a Salpeter IMF in the mass range $1 - 100 M_\odot$. With this assumption, the parameter $N_{\rm ion}$ will be given by

$$N_{\rm ion} \approx 3200 \epsilon_{*,{\rm II}} f_{\rm esc,II} = 3200 \epsilon_{\rm II}, \quad (3)$$

where we have defined $\epsilon_{\rm II} \equiv \epsilon_{*,{\rm II}} f_{\rm esc,II}$. We assume $\epsilon_{\rm II}$ to be independent of redshift and consider it as a free parameter in our model. In this work, we do not invoke any other sources of reionization which are often done in other studies, e.g., metal-free PopIII stars. Our main aim would be to verify if the presence of magnetic fields is able to eliminate the requirement of PopIII stars and still give a good match to the data.

The collapse fraction, $f_{\rm coll}$, depends on the minimum mass of star-forming haloes. In neutral regions, we assume it to be determined by atomic cooling (i.e. we neglect cooling through molecular hydrogen). However, the minimum mass will be larger in ionized regions because of radiative feedback. Our model can compute radiative feedback (suppressing star formation in low-mass haloes using a Jeans mass prescription) self-consistently from the evolution of the thermal properties of the IGM. The corresponding filtering scale, which depends on the temperature evolution of the IGM, is found to be typically around ~ 30 km s^{-1}.

The HI photoionization rate is given by

$$\Gamma_{\rm HI}(z) = 4\pi(1+z)^3 \int_{\nu_{\rm HI}} {\rm d}\nu \; \lambda_{\rm mfp}(z,\nu) \; \dot{n}_{z,\nu} \; \sigma_{\rm HI}(\nu), \quad (4)$$

where $\sigma_{\rm HI}$ is the photoionization cross section and $\lambda_{\rm mfp}$ is the mean free path of ionizing photons. The mean free path is modelled as (Miralda-Escudé, Haehnelt, & Rees 2000)

$$\lambda_{\rm mfp}(z) = \frac{\lambda_0}{[1 - F_V(z)]^{2/3}}, \quad (5)$$

where F_V is the volume fraction of ionized regions and λ_0 is a normalization parameter. This parameter can be constrained using the redshift distribution of Lyman-limit systems

$$\frac{{\rm d}N_{\rm LL}}{{\rm d}z} = \frac{c}{\sqrt{\pi}\lambda_{\rm mfp}(z) H(z) (1+z)}. \quad (6)$$

Given a reionization history, we compute the angular power spectra C_l of CMB temperature and (E-mode) polarization anisotropies. We combine our calculations with the publicly available code CAMB[3] (Lewis, Challinor, & Lasenby 2000) in order to do so. The crucial parameter which determines the C_l is the electron scattering optical depth

$$\tau_{\rm el}(z) = \sigma_T c \int_0^{t(z)} {\rm d}t \; n_e(z) \; (1+z)^3, \quad (7)$$

where $n_e(z)$ is the comoving number density of free electrons and σ_T is the Thomson cross section and c is the speed of light.

2.1 Inclusion of magnetic fields

The effect of the magnetic field is included by adding the additional matter power induced by these fields to the usual dark matter power spectrum $P_{\rm DM}(k)$. As we show below, the collapsed fraction $f_{\rm coll}$, which determines the ionizing emissivity in equation (1), is a sensitive function of $P_{\rm DM}(k)$ and hence the inclusion of magnetic fields can significantly alter the reionization history.

[3] `http://camb.info/`

We assume the primordial magnetic field to be a stochastic Gaussian field (see Mack, Kahniashvili, & Kosowsky 2002 and references therein). For a non-helical magnetic field, the two-point correlation function of the tangled field can be written as:

$$\langle B_i^\star(\mathbf{k}) B_j(\mathbf{k}')\rangle = (2\pi)^3 \delta^{(3)}(\mathbf{k}-\mathbf{k}') P_{ij}(\hat{\mathbf{k}}) P_{\rm B}(k). \quad (8)$$

Here i and j are spatial indices, $i,j \in (1,2,3)$, $\hat{k}_i = k_i/k$ a unit wave vector, $P_{ij}(\hat{\mathbf{k}}) = \delta_{ij} - \hat{k}_i\hat{k}_j$ the transverse plane projector, $\delta^{(3)}(\mathbf{k}-\mathbf{k}')$ the Dirac delta function, and $P_{\rm B}(k) = Ak^{n_{\rm B}}$ is the power spectrum of the magnetic field; here A normalizes the power in magnetic fields and $n_{\rm B}$ is the spectral index. The parameter A is computed by defining the RMS of magnetic field at cut off scale k_c; the RMS for $k_c = 1\,{\rm Mpc}^{-1}$, is referred to as the magnetic field strength, B_0 (Mack, Kahniashvili, & Kosowsky 2002). The relation between A and B_0 is given by

$$A = \frac{(2\pi)^{n_{\rm B}+5} B_0^2}{2\Gamma(n_{\rm B}/2+3/2)}. \quad (9)$$

The magnetic field power spectrum drops at small scales owing to dissipation in the pre-recombination era. The cut-off scale $k_{\rm max}$ is determined by the Alfvén wave damping scale $k_{\rm max}^{-1} \sim v_A L_S$ where v_A is the Alfvén velocity and L_S the Silk damping scale (Jedamzik, Katalinić, & Olinto 1998): $k_{\rm max} \simeq 200\,(1\,{\rm nG}/B_0)\,{\rm Mpc}^{-1}$.

The primordial magnetic field induces density perturbations in the post-recombination era which grow by gravitational collapse (Wasserman 1978, Kim, Olinto, & Rosner 1996, Gopal & Sethi 2003). The matter power spectrum induced by magnetic fields has the shape: $P(k) \propto k^{2n_{\rm B}+7}$ for $n_{\rm B} \leq -1.5$; this matter power spectrum is cut off at the magnetic field Jeans' scale: $k_J \simeq 15(1\,{\rm nG}/B_0)\,{\rm Mpc}^{-1}$ (Kim, Olinto, & Rosner 1996, Gopal & Sethi 2003) [4]. The matter power spectrum is shown in the Figure 1 for different values of B_0 and $n_{\rm B}$ along with the power spectrum for the usual ΛCDM case. As shown in the Figure, we adopt a sharp cut-off of the matter power spectrum at the magnetic Jeans' scale $k = k_J$ (Peebles 1980; Sethi & Subramanian 2005; Tashiro & Sugiyama 2006a; Tashiro & Sugiyama 2006b; Schleicher et al. 2009; Tashiro & Sugiyama 2011; Schleicher & Miniati 2011; Tashiro, Takahashi, & Ichiki 2012; Pandey & Sethi 2012). We note that the mass dispersion $\sigma^2 \propto k^3 P(k)$ and the number of haloes for a given mass is very sensitive to σ. Therefore, by adopting a sharp cut-off, we obtain conservative limits on the strength of magnetic field as compared to the case in which the cut-off is gradual (Pandey & Sethi 2013).

It has been shown from other cosmological observables that the only class of acceptable magnetic field models correspond to the near scale-free models, $n_{\rm B} \simeq -3$ (e.g. Sethi & Subramanian 2005). Hence in this work we study only models with $n_{\rm B}$ very close to -3.

In this paper we assume the sources of inflationary density perturbations and magnetic field generation to be uncorrelated. This allows us to add the two matter power spectra in quadrature for our computation. It should also be underlined that the presence of sub-nG fields does not substantially change the normalization of σ_8, as magnetic field induced matter power spectra make negligible contribution to the scales of interest: $k \simeq 0.01$–$0.5\,{\rm Mpc}^{-1}$ (Figure 1). As noted above, the main impact of the extra matter power induced by magnetic fields is to increase the collapse fraction and alter its evolution. This induced power spectrum (Figure 1) causes collapse of mass haloes close to the magnetic field Jeans' scale (e.g. Kahniashvili et al. 2010) and therefore changes ionization history which might not be reproducible by altering parameters within the framework of ΛCDM model.

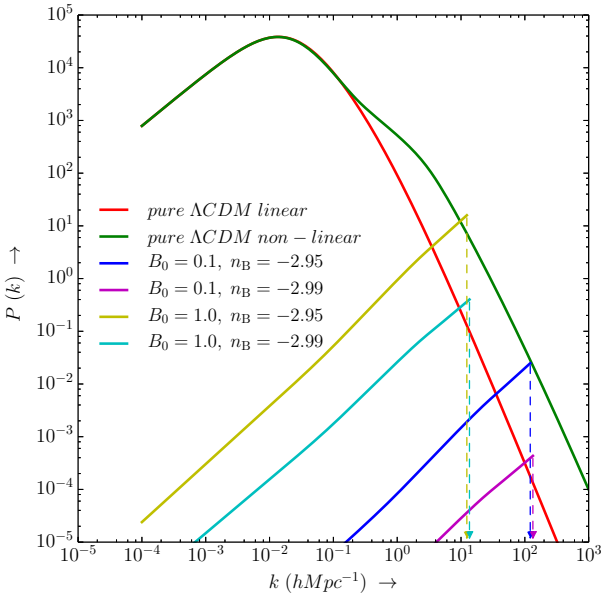
pure ΛCDM linear
pure ΛCDM non − linear
$B_0 = 0.1,\ n_{\rm B} = -2.95$
$B_0 = 0.1,\ n_{\rm B} = -2.99$
$B_0 = 1.0,\ n_{\rm B} = -2.95$
$B_0 = 1.0,\ n_{\rm B} = -2.99$
$P\ (k)\ \rightarrow$
$k\ (hMpc^{-1})\ \rightarrow$

Figure 1. Inflationary and primordial magnetic field induced matter power spectra. A sharp cut-off has been put at the magnetic Jeans scale for magnetic cases.

3 RESULTS

3.1 Free parameters

In this section, we present the results of our calculation. We work with a flat ΛCDM cosmological model defined by five parameters $\Omega_m, \Omega_b, h, \sigma_8, n_s$. This has to be supplemented by the two parameters related to reionization, the stellar efficiency parameter $\epsilon_{\rm II}$ and the normalization of the mean free path λ_0. For models with magnetic field, we need two more free parameters B_0 and $n_{\rm B}$ to complete the set.

It has been shown that among the cosmological parameters, the two which affect the reionization history most significantly are the ones related to the dark matter fluctuation power spectrum, i.e. σ_8, n_s. In fact, even when the three parameters Ω_m, Ω_b, h are kept fixed, it is found that the best-fit values and the error-bars on the parameters $\epsilon_{\rm II}$ and λ_0 remain almost identical to the case when all the parameters are allowed to vary (Mitra, Choudhury, & Ferrara 2012). For the rest of the paper, we thus fix the values of these parameters to their WMAP9 best-fit values $\Omega_m = 0.279, \Omega_b = 0.046, h = 0.70$ (Bennett et al. 2013).[5]

[4] The quantity $k_{\rm max}$ is a cut-off scale in magnetic field power spectrum $P_{\rm B}(k)$ in eq 8, whereas k_J is a magnetic Jeans cut-off scale in magnetic field induced matter power spectrum due to magnetic pressure. The magnetic Jeans scale does depend on $n_{\rm B}$, but the dependence is extremely weak for near scale-free models $n_{\rm B} \simeq -3$.

[5] One may argue that it is more reasonable to use priors from more

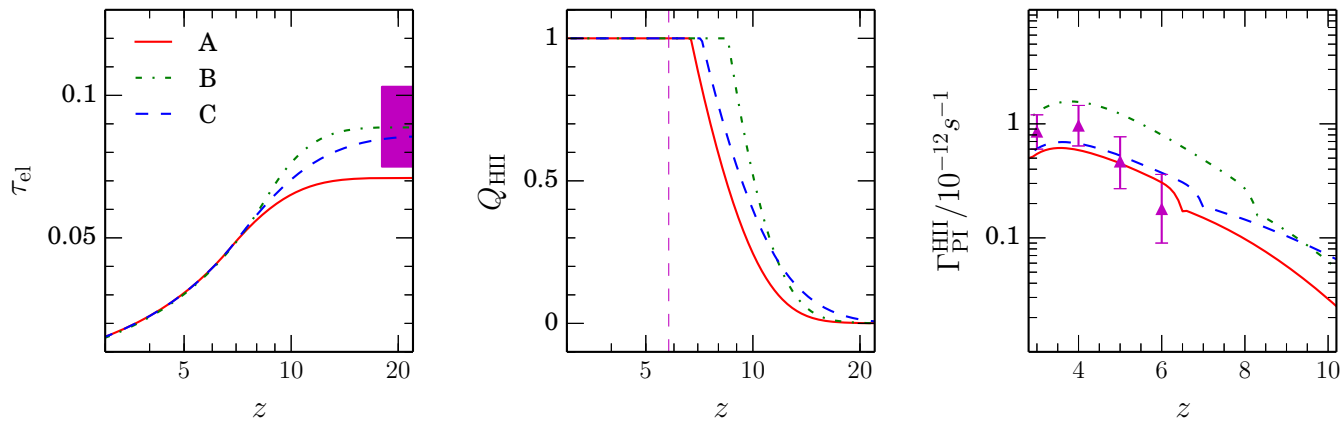

Figure 2. Effect of non-zero B_0 on quantities related to reionization. The left hand panel shows the evolution of electron scattering optical depth $\tau_{\rm el}$, the middle panel shows the volume filling factor of ionized regions and the right hand panel shows the evolution of the photoionization rate $\Gamma_{\rm HI}$. We have also shown the observational data points, see text for details. The three models shown are summarized in Table 1.

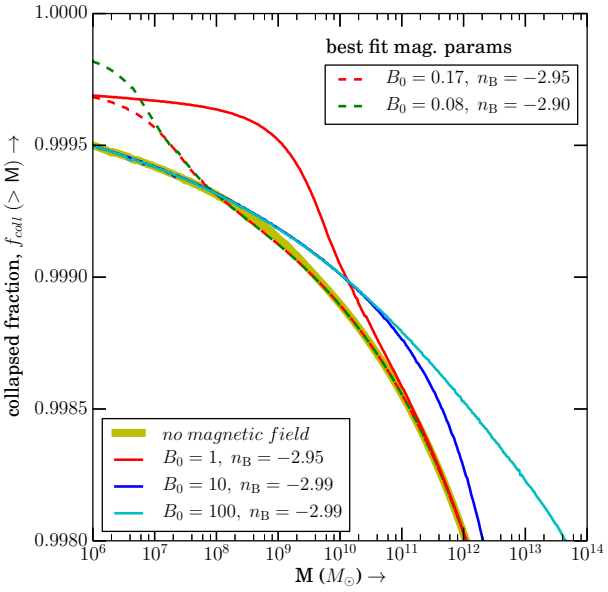
best fit mag. params
$B_0 = 0.17,\ n_B = -2.95$
$B_0 = 0.08,\ n_B = -2.90$
no magnetic field
$B_0 = 1,\ n_B = -2.95$
$B_0 = 10,\ n_B = -2.99$
$B_0 = 100,\ n_B = -2.99$
collapsed fraction, f_{coll} (> M) →
M ($M_\odot$) →

Figure 3. Collapsed fraction $f_{\rm coll}(> M)$ of haloes having mass greater than M for $z = 10$. Magnetic field values shown in the figure are in units of nG. The dashed lines are for the values of B_0 and $n_{\rm B}$ which are close to the best-fit values obtained from reionization constraints.

recent experiments like Planck (Planck Collaboration et al. 2013b). We use the WMAP9 priors mainly because the data and likelihood analysis used in section 3.3 are from WMAP9. Using data from Planck Collaboration et al. (2013b) may not alter the constraints obtained in this work as most of the parameters have almost similar values (the value of h is smaller for Planck than WMAP, however the combination $\Omega_m h^2$ remains almost similar, and hence the effect on reionization is not that drastic). It might be interesting to revisit this problem once the Planck polarization measurements are released.

Parameter	Model A	Model B	Model C
B_0 (nG)	0.0	0.0	0.08
$\epsilon_{\rm II}$	0.006	0.0175	0.006

Table 1. Models used for discussing the effect of B_0 on reionization history.

3.2 Effect of magnetic fields on reionization history

We first discuss the effects of non-zero magnetic field on the reionization history. In addition to fixing Ω_m, Ω_b, h as mentioned above, we fix the values of the cosmological parameters $\sigma_8 = 0.821, n_s = 0.972$ to their best-fit values, and also fix $n_{\rm B} = -2.9$. The arguments presented in this section would hold equally well for any other value of $n_{\rm B}$ close to -3. It is sufficient to vary the efficiency parameter $\epsilon_{\rm II}$ and the magnetic field B_0 to understand the effect. The models and the parameters considered in this subsection are summarized in Table 1.

We plot the evolution of the electron scattering optical depth $\tau_{\rm el}$, the volume filling factor of ionized regions $Q_{\rm HII}$ and the hydrogen photoionization rate $\Gamma_{\rm HI}$ in Figure 2. We also compare the models with relevant observational data, i.e., with the WMAP9 constraints on $\tau_{\rm el}$ (Bennett et al. 2013) and the measurements of $\Gamma_{\rm HI}$ from Lyα forest data (Wyithe & Bolton 2011; Becker & Bolton 2013). Consider first model A, which has no magnetic field. The value of $\epsilon_{\rm II}$ is chosen such that it is consistent with the upper limits of $\Gamma_{\rm HI}$ measurements at $z = 6$ (right hand panel), i.e., this is the largest $\epsilon_{\rm II}$ consistent with the Lyα forest data. The left hand panel shows that this model underpredicts the value of $\tau_{\rm el}$ given by the WMAP9 observations. If we try to match the $\tau_{\rm el}$ constraints without introducing any additional physics, we have to increase the value of $\epsilon_{\rm II}$. Model B represents such a scenario where $\epsilon_{\rm II}$ has been increased by a factor of ~ 3 compared to A. Now the match with $\tau_{\rm el}$ is quite good, however, this model overpredicts the $\Gamma_{\rm HI}$ at $z = 6$ by a large amount[6].

We now introduce a non-zero magnetic field $B_0 = 0.08$ nG

[6] Of course, the tension between these two data sets can be reconciled if it is found that the value of $\tau_{\rm el}$ inferred by WMAP is higher

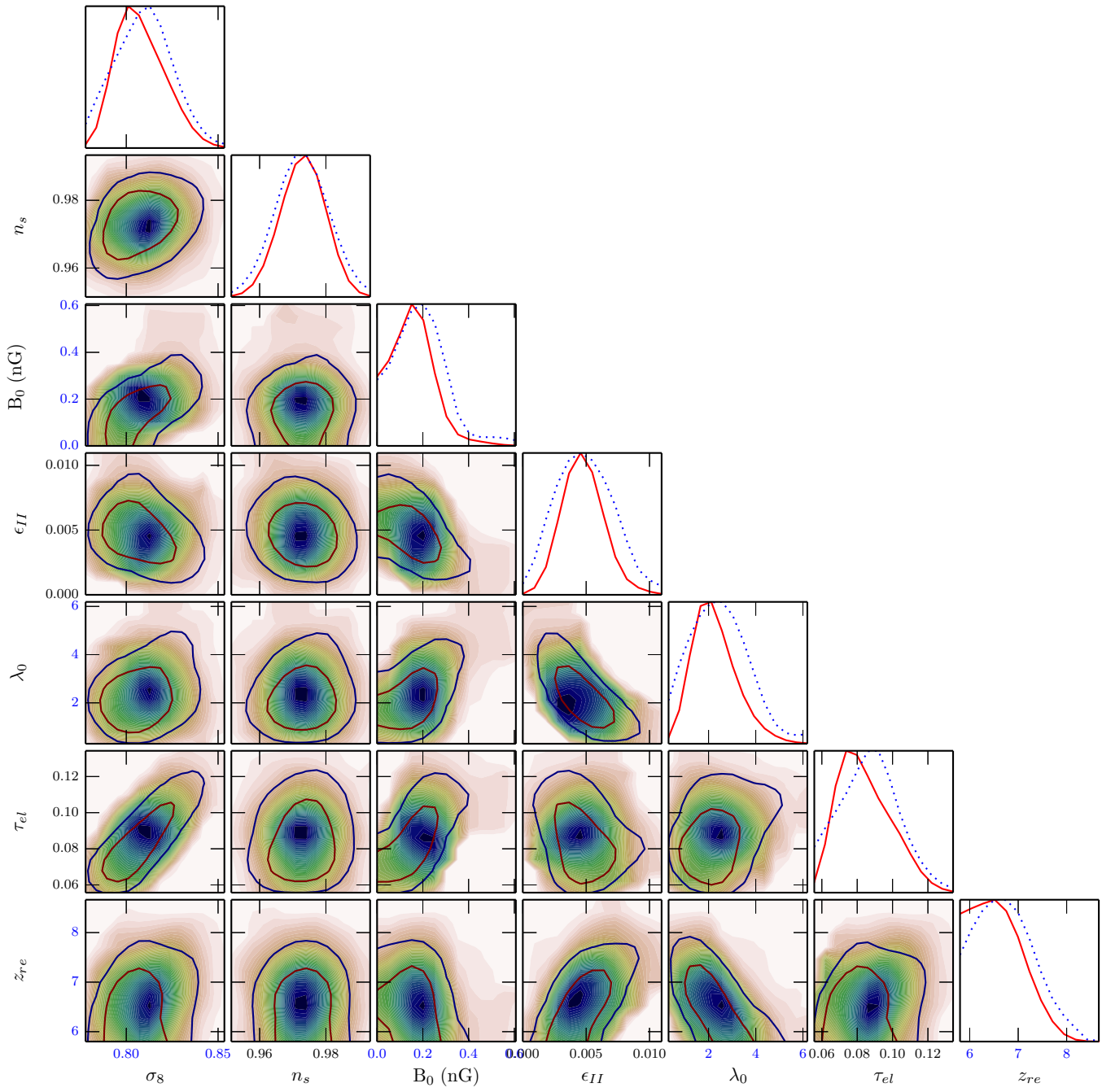

Figure 4. Likelihood constraints for $n_{\rm B} = -2.95$. The contours are drawn at 68% and 95% confidence level. The solid and the dashed curves in the diagonal plots are respectively, the marginalised posterior probability distribution and normalized mean likelihoods of the corresponding parameter.

(with $n_{\rm B} = -2.9$) in our model. It is possible to repeat the following exercise with any other value of $n_{\rm B}$ by choosing an appropriate B_0. The efficiency parameter in model C is kept identical to model A. We now see that the model is able to match both the $\Gamma_{\rm HI}$ data at $z = 6$ and the $\tau_{\rm el}$ constraints. This shows that magnetic field can be useful in relieving the tension between the CMB and QSO absorption line data sets. The main reason for this is that presence of magnetic field allows for early formation of galaxies and hence can drive early reionization. However, as reionization progresses, the radiative feedback effects become more important and regulates the formation of ionizing sources at $z \sim 10$. This leads to a feedback-regulated, extended and photon-starved reionization which is required for good match with the data (Bolton & Haehnelt 2007; Mitra, Choudhury, & Ferrara 2011; Mitra, Choudhury, & Ferrara 2012)[7]. It also follows that this

than the true value, as is evident from the latest Planck results (Planck Collaboration 2015)

[7] There are alternate ways to achieve a reionization model which is consistent with all the data sets, e.g., by introducing star for-

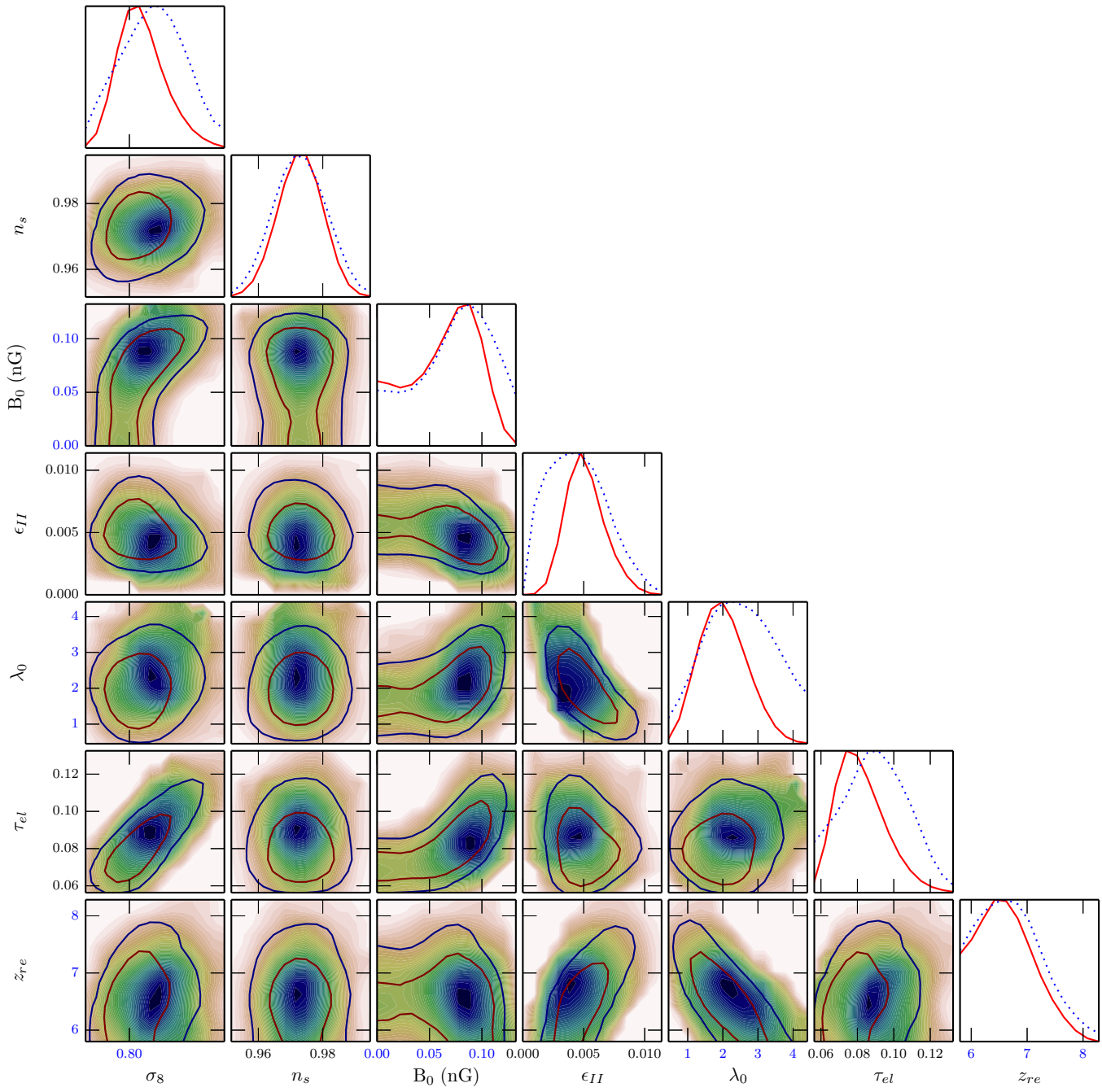

Figure 5. Likelihood constraints for $n_{\rm B} = -2.90$. The contours are drawn at 68% and 95% confidence level. The solid and the dashed curves in the diagonal plots are respectively, the marginalised posterior probability distribution and normalized mean likelihoods of the corresponding parameter.

set of observations can also be used to put constraints on B_0 as too high a value of B_0 would lead to reionization too early and would violate the $\tau_{\rm el}$ bounds.

In Figure 3, we show the collapsed fraction for different values of B_0 and the spectral index $n_{\rm B}$. This figure allows us to understand the results of the current and the next section where we present detailed multi-parameter analysis. As noted above, the main impact of the primordial magnetic fields is to enhance density fluctuations at small scales (Figure 1). Figure 3 shows the impact of this addition to the collapsed fraction as a function of mass. The collapsed fraction is seen to be a sensitive and complex function of the parameter associated with primordial magnetic fields.

We could understand this dependence as follows. For the magnetic field-induced density perturbations, the mass dispersion at a given scale: $\sigma(M) \propto B_0^2(n_{\rm B}+3)$ (Vasiliev & Sethi 2014). Also $\sigma(M) \propto M^{-2/3}$ above the magnetic field Jeans' scale which is a sharper fall as compared to

mation within minihaloes (Choudhury, Ferrara, & Gallerani 2008) or by including a population of metal-free stars at high redshifts (Choudhury & Ferrara 2006).

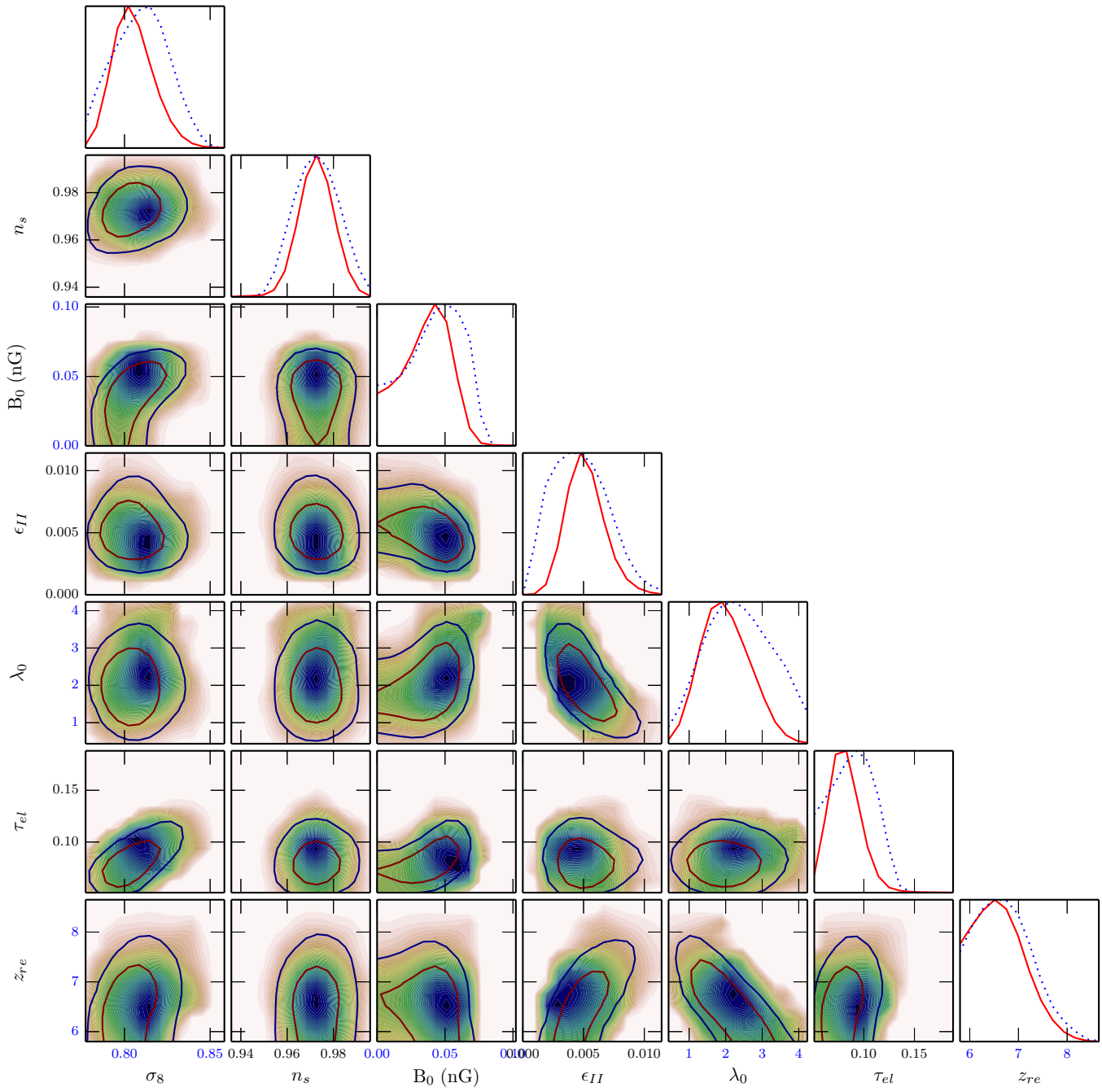

Figure 6. Likelihood constraints for $n_{\rm B} = -2.85$. The contours are drawn at 68% and 95% confidence level. The solid and the dashed curves in the diagonal plots are respectively, the marginalised posterior probability distribution and normalized mean likelihoods of the corresponding parameter.

the ΛCDM model in the relevant mass range. This also means that the collapsed fraction is dominated by a small range of mass scales around the magnetic field Jeans' scale (see e.g. Vasiliev & Sethi 2014, Figure 3). In the Press-Schechter formalism used to compute the collapsed fraction, the fraction increases with $\sigma(M)$ and could be exponentially sensitive to the mass dispersion. Therefore, we expect an increase in the mass fraction as $n_{\rm B}$ is increased for a fixed B_0. A change in the value of B_0 results in two distinct effects: (i) $\sigma(M)$ increases which tends to increase the collapsed fraction (ii) the magnetic Jeans' length also increases (for details see discussion in section 2.2) which tends to decrease the collapsed fraction below the magnetic field Jeans' mass. The net effect of increasing the value of B_0 is to shift the collapsed fraction to larger masses while decreasing the fraction at smaller masses, as seen in Figure 3.

3.3 Constraints on B_0

In this section, we present results related to the constraints on B_0 based on detailed multi-parameter MCMC analysis.

We have modified the publicly available code COSMOMC[8] (Lewis & Bridle 2002) to account for generic reionization histories (Mitra, Choudhury, & Ferrara 2011; Pandolfi et al. 2011) and the effect of magnetic field on the matter power spectrum. We take three different values of $n_{\rm B} = -2.95, -2.90, -2.85$ and for each case we vary five parameters, namely, $\sigma_8, n_s, B_0, \epsilon_{\rm II}, \lambda_0$, keeping all the rest of the parameters fixed. We constrain these parameters using (i) the WMAP9 data on angular power spectra corresponding to the temperature autocorrelation (TT), the E-mode polarization autocorrelation (EE) and the TE cross-correlation (Bennett et al. 2013), (ii) the photoionization rate in the IGM inferred from the Lyα forest at $z \leq 6$ (Wyithe & Bolton 2011; Becker & Bolton 2013) and (iii) the redshift distribution of Lyman-limit systems at $z < 6$ (Songaila & Cowie 2010).

We would like to mention here that, we tried case $n_{\rm B} = -2.99$ too but it turned out that the effect of magnetic field on the mass function of collapsed haloes is negligible in the mass scales relevant for reionization. The reason is that the magnetic field-induced mass fluctuations have the dependence $\sigma(M) \propto B_0^2(n_{\rm B}+3)$, and hence one requires very high value of B_0 to obtain any significant effect when $n_{\rm B} \to -3$. The collapsed mass fraction $f_{\rm coll}(>M)$ for $B_0 \sim 1$ nG is almost same as the non-magnetic case for $M \lesssim 10^{12}$ M$_\odot$, see Figure 3, thus implying that no significant effect on reionization history can be expected. If we try to increase the collapse mass fraction by making magnetic field value very high, the effect starts to show at very large scales (e.g., $B_0 \sim 100$ nG shows significant effects only for $M \gtrsim 10^{12}$ M$_\odot$). The reason for this is that magnetic Jeans cut-off scale is roughly proportional to the magnetic field strength ($k_J \propto B_0^{-1}$). Since the contribution of high mass haloes to the total ionizing photon budget is negligible, they hardly make any difference to the reionization history. Consequently the magnetic field seems to play no role for $n_{\rm B} = -2.99$. This also suggests that the reionization starts to become insensitive to magnetic field effects as $n_{\rm B} \to -3$.

We show the results for three fixed values of $n_{\rm B}$: Figure 4 shows the likelihood contours for $n_{\rm B} = -2.95$ (which is almost scale-free). The contours for $n_{\rm B} = -2.90$ are shown in Figure 5 and the ones for $n_{\rm B} = -2.85$ are shown in Figure 6. The results of our analysis are summarized in Table 2. Note that in these figures and the tables, the parameter z_{re} refers to the redshift when the reionization is 99% complete as given by our detailed model of reionization.

We can understand our main results based on the discussion in the previous subsection. The upper limit on B_0 lies in the range 0.36–0.06 nG and this limit decreases as $n_{\rm B}$ is increased in the range $n_{\rm B} = -2.95$ to -2.85, as we expect from the discussion in the previous subsection. We note from the figures that B_0 is anti-correlated with the two parameters $\epsilon_{\rm II}$ and λ_0. This is expected as a decrease in $\epsilon_{\rm II}$ which results in inefficient production of ionizing photons which can be compensated by an increase in B_0 leading to early halo formation. Similarly a decrease in λ_0 leads to smaller values of the photoionization rate which too can be compensated by a higher B_0. It is also not surprising that B_0 is strongly correlated with the derived parameter $\tau_{\rm el}$, as larger values of B_0 leads to early reionization and hence larger $\tau_{\rm el}$.

Our analysis shows (Table 2) that the best-fit value of B_0 is always non-zero, i.e., one obtains a better match to the data when a non-zero magnetic field is included in the reionization model. However, it is not possible to rule out the non-magnetic cases within 2-σ limits. We also find that the inferred values of the cosmological parameters σ_8 and n_s are quite close to what obtained by the WMAP9 team (Bennett et al. 2013).

We discuss some of the caveats for our analysis. The magnetic Jeans' scale play a crucial role in our analysis. The fact that the magnetic Jeans' scale is not a very well defined quantity like the thermal Jeans' scale as it indicates the breakdown of linear analysis in a magnetized fluid (Kim, Olinto, & Rosner 1996), there is an inherent leverage in our analysis. However, as we have discussed in the section 2.1, we take a conservative approach by taking a sharp cut-off at magnetic Jeans' scale k_J, the constraints on B_0 would be even tighter if we use a gradual cut-off. In the reionization model studied here, the assumption of a redshift-independent $\epsilon_{\rm II}$ is used. Some of the constraints on B_0 might change if this assumption is relaxed. For example, if the effective $\epsilon_{\rm II}$ is allowed to increase at high redshifts (e.g., introducing a population of metal-free stars and/or X-ray ionizing sources), then the upper-limit on B_0 would become much tighter. On the other hand, if there are reasons to believe that $\epsilon_{\rm II}$ decreases at high-z (e.g., if the escape fraction of photons is less at early epochs), then one would need higher values of B_0 to explain the data and hence the upper-limit on B_0 would be weaker. Interestingly, one may end up putting a lower-limit on B_0 in such a case. Similarly, the constraints on B_0 could be degenerate with the effects of feedback. In this work, we have used a simple model of radiative feedback based on Jeans prescription, while the actual situations could be more complex. It would be interesting to check how the constraints change with different prescriptions for feedback. The other crucial assumption in our work is that we ignore the possibility of molecular cooling in haloes. If such an effect is introduced, it will allow star formation in minihaloes and would thus favour early reionization. In that case we would be able to put much tighter limits on B_0. We shall explore such interesting possibilities in a later work.

4 DISCUSSION

We studied the possible role primordial magnetic fields might play in explaining the reionization history of the universe in the redshift range $z \simeq 6$–10. These fields enhance the power in the dark matter density fluctuations at small scales thus allowing early structure formation. Our main results are: (i) a non-zero B_0 helps in relieving the tension between CMB and quasar absorption line data sets in the photon-starved reionization scenario by enabling early structure formation, and (ii) the data sets can be useful in putting a upper-limit on B_0, we obtain $B_0 < 0.358, 0.120, 0.059$ nG (95 % c.l.) for $n_{\rm B} = -2.95, -2.9, -2.85$, respectively.

Many cosmological observables have been analysed to constrain the amplitude and the spectral index of the magnetic field power spectrum: CMB observations, early structure formation, weak gravitational lensing, Lyman-α data, etc.; these considerations put upper bounds on B_0 in the range 0.3–1 nG (e.g. Trivedi, Seshadri, & Subramanian 2012, Kahniashvili et al. 2010, Shaw & Lewis 2012, Pandey & Sethi 2013, Pandey & Sethi 2012, Lewis 2004, Caprini, Durrer, & Kahniashvili 2004). Bounds obtained from Big Bang Nucleosynthesis constraints give $B_0 \lesssim 10^{-7}$ G (Suh & Mathews 1999). Earlier constraints on primordial magnetic fields coming from the study of ionization history of the

[8] `http://cosmologist.info/cosmomc`

Parameter	$n_{\rm B} = -2.95$			$n_{\rm B} = -2.90$			$n_{\rm B} = -2.85$		
	Best-fit	Mean	95% c.l.	Best-fit	Mean	95% c.l.	Best-fit	Mean	95% c.l.
σ_8	0.811	0.808	[0.786, 0.837]	0.810	0.806	[0.787, 0.838]	0.809	0.805	[0.787, 0.835]
n_s	0.972	0.973	[0.959, 0.986]	0.974	0.973	[0.960, 0.985]	0.973	0.973	[0.960, 0.968]
B_0 (nG)	0.189	0.159	< 0.358	0.081	0.065	< 0.120	0.048	0.036	< 0.059
$\epsilon_{\rm II}$	0.0042	0.0048	[0.0022, 0.0090]	0.0051	0.0052	[0.0028, 0.0086]	0.0043	0.0052	[0.0030, 0.0087]
λ_0	2.337	2.273	[0.918 , 4.541]	1.817	2.021	[0.944, 4.093]	2.233	2.008	[0.901, 3.721]
$\tau_{\rm el}$	0.089	0.084	[0.063 , 0.118]	0.086	0.082	[0.063, 0.119]	0.085	0.082	[0.063, 0.119]
$z_{\rm re}$	6.400	6.579	[5.800 , 7.800]	6.800	6.628	[5.800, 7.600]	6.400	6.624	[5.800, 7.800]
χ^2	3781.18	–	–	3781.23	–	–	3781.18	–	–

Table 2. Parameter constraints

post-recombination universe (Tashiro & Sugiyama 2006a, Schleicher, Banerjee, & Klessen 2008, Schleicher & Miniati 2011) also put the upper bound on B_0 in the reange 0.7–5 nG. Our results are consistent with all these constraints. Interestingly, even magnetic fields of smaller magnitude $\simeq 0.1$ nG can have an appreciable and potentially detectable impact on the reionization history. In the future, one can possibly improve these bounds by understanding some of the physical processes related to reionization (e.g., feedback) through detailed modelling.

REFERENCES

Ashoorioon A., Mann R. B., 2005, Phys. Rev. D, 71, 103509
Beck R., 2012, Space Sci. Rev., 166, 215
Becker G. D., Bolton J. S., 2013, MNRAS, 436, 1023
Bennett C. L. et al., 2013, ApJS, 208, 20
Bolton J. S., Haehnelt M. G., 2007, MNRAS, 382, 325
Caprini C., Durrer R., Kahniashvili T., 2004, Phys. Rev. D, 69, 063006
Chongchitnan S., Meiksin A., 2014, MNRAS, 437, 3639
Choudhury T. R., 2009, Current Science, 97, 841
Choudhury T. R., Ferrara A., 2005, MNRAS, 361, 577
Choudhury T. R., Ferrara A., 2006, MNRAS, 371, L55
Choudhury T. R., Ferrara A., Gallerani S., 2008, MNRAS, 385, L58
Fan X. et al., 2006, AJ, 132, 117
Gopal R., Sethi S. K., 2003, Journal of Astrophysics and Astronomy, 24, 51
Jedamzik K., Katalinić V., Olinto A. V., 1998, Phys. Rev. D, 57, 3264
Kahniashvili T., Tevzadze A. G., Sethi S. K., Pandey K., Ratra B., 2010, Phys. Rev. D, 82, 083005
Kim E.-J., Olinto A. V., Rosner R., 1996, ApJ, 468, 28
Kim K.-T., Kronberg P. P., Giovannini G., Venturi T., 1989, Nature, 341, 720
Lewis A., 2004, Phys. Rev. D, 70, 043011
Lewis A., Bridle S., 2002, Phys. Rev. D, 66, 103511
Lewis A., Challinor A., Lasenby A., 2000, ApJ, 538, 473
Mack A., Kahniashvili T., Kosowsky A., 2002, Phys. Rev. D, 65, 123004
Miralda-Escudé J., Haehnelt M., Rees M. J., 2000, ApJ, 530, 1
Mitra S., Choudhury T. R., Ferrara A., 2011, MNRAS, 413, 1569
Mitra S., Choudhury T. R., Ferrara A., 2012, MNRAS, 419, 1480
Pandey K. L., Sethi S. K., 2012, ApJ, 748, 27
Pandey K. L., Sethi S. K., 2013, ApJ, 762, 15
Pandolfi S., Ferrara A., Choudhury T. R., Melchiorri A., Mitra S., 2011, Phys. Rev. D, 84, 123522
Parker E. N., 1979, Cosmical magnetic fields: Their origin and their activity
Peebles P. J. E., 1980, The large-scale structure of the universe
Planck Collaboration , 2015, ArXiv e-prints, 1502, 1589
Planck Collaboration et al., 2013a, ArXiv e-prints
Planck Collaboration et al., 2013b, ArXiv e-prints
Ratra B., 1992, ApJ, 391, L1
Ryu D., Schleicher D. R. G., Treumann R. A., Tsagas C. G., Widrow L. M., 2012, Space Sci. Rev., 166, 1
Schleicher D. R. G., Banerjee R., Klessen R. S., 2008, Phys. Rev. D, 78, 083005
Schleicher D. R. G., Galli D., Glover S. C. O., Banerjee R., Palla F., Schneider R., Klessen R. S., 2009, ApJ, 703, 1096
Schleicher D. R. G., Miniati F., 2011, MNRAS, 418, L143
Sethi S. K., Subramanian K., 2005, MNRAS, 356, 778
Sethi S. K., Subramanian K., 2009, J. Cosmology Astropart. Phys., 11, 21
Shaw J. R., Lewis A., 2012, Phys. Rev. D, 86, 043510
Songaila A., Cowie L. L., 2010, ApJ, 721, 1448
Suh I.-S., Mathews G. J., 1999, Phys. Rev. D, 59, 123002
Tashiro H., Sugiyama N., 2006a, MNRAS, 368, 965
Tashiro H., Sugiyama N., 2006b, MNRAS, 372, 1060
Tashiro H., Sugiyama N., 2011, MNRAS, 411, 1284
Tashiro H., Takahashi K., Ichiki K., 2012, MNRAS, 424, 927
Trivedi P., Seshadri T. R., Subramanian K., 2012, Physical Review Letters, 108, 231301
Turner M. S., Widrow L. M., 1988, Phys. Rev. D, 37, 2743
Vasiliev E. O., Sethi S. K., 2014, ApJ, 786, 142
Wasserman I., 1978, ApJ, 224, 337
Widrow L. M., 2002, Reviews of Modern Physics, 74, 775
Wyithe J. S. B., Bolton J. S., 2011, MNRAS, 412, 1926
Yamazaki D. G., 2014, Phys. Rev. D, 89, 083528
Yamazaki D. G., Kajino T., Mathews G. J., Ichiki K., 2012, Phys. Rep., 517, 141
Zeldovich I. B., Ruzmaikin A. A., Sokolov D. D., ed, 1983, Magnetic fields in astrophysics, Vol. 3